

# Cores in warm dark matter haloes: a *Catch 22* problem

Andrea V. Macciò<sup>1\*</sup>, Sinziana Paduroiu<sup>2</sup>, Donnino Anderhalden<sup>3</sup>  
Aurel Schneider<sup>3</sup>, Ben Moore<sup>3</sup>

<sup>1</sup> *Max-Planck-Institute for Astronomy, Königstuhl 17, D-69117 Heidelberg, Germany*

<sup>2</sup> *Geneva Observatory, University of Geneva, CH-1290 Sauverny, Switzerland*

<sup>3</sup> *Institute for Theoretical Physics, University of Zürich, CH-8057 Zürich, Switzerland*

8 February 2012

## ABSTRACT

The free streaming of warm dark matter particles dampens the fluctuation spectrum, flattens the mass function of haloes and imprints a fine grained phase density limit for dark matter structures. The phase space density limit is expected to imprint a constant density core at the halo center on the contrary to what happens for cold dark matter. We explore these effects using high resolution simulations of structure formation in different warm dark matter scenarios. We find that the size of the core we obtain in simulated haloes is in good agreement with theoretical expectations based on Liouville’s theorem. However, our simulations show that in order to create a significant core, ( $r_c \sim 1$  kpc), in a dwarf galaxy ( $M \sim 10^{10} M_\odot$ ), a thermal candidate with a mass as low as 0.1 keV is required. This would fully prevent the formation of the dwarf galaxy in the first place. For candidates satisfying large scale structure constraints ( $m_\nu$  larger than  $\approx 1 - 2$  keV) the expected size of the core is of the order of 40 (80) pc for a dark matter halo with a mass of  $10^{10}$  ( $10^8$ )  $M_\odot$ . We conclude that “standard” warm dark matter is not viable solution for explaining the presence of cored density profiles in low mass galaxies.

## Key words:

Dark matter: N-body simulations – galaxies, haloes.

## 1 INTRODUCTION

The formation of structure in the universe is driven by the mysterious dark matter component whose nature is still unknown. Over the last decades, the hierarchical cold dark matter model (CDM) has become the standard description for the formation of cosmic structures. It is in excellent agreement with recent observations, such as measurements of the cosmic microwave background and large scale surveys (Tegmark et al. 2006; Komatsu et al. 2011). However, there are a number of inconsistencies on sub-galactic scales that arise within the CDM scenario. Firstly, the amount of substructure in Milky Way sized haloes is overpredicted by roughly one order of magnitude (Klypin et al. 1999; Moore et al. 1999). Secondly, the central densities of CDM haloes in simulations show a cuspy behavior (Moore 1994; Flores & Primack 1994; Diemand et al. 2005; Macciò et al. 2007; Springel et al. 2008), whereas the density profiles inferred from galaxy rotation curves point to a core like structure (e.g. de Blok et al. 2001;

Kuzio de Naray et al. 2009; Oh et al. 2011). Furthermore, recent studies (Tikhonov et al. 2009; Zavala et al. 2009; Peebles & Nusser 2010) re-emphasized that also the population of dwarf galaxies within voids is in strong contradiction with CDM predictions.

One possible solution to these issues is that the dark matter particle is a thermal relic with a mass of order one keV. The most prominent representatives of such warm dark matter (WDM) candidates are the sterile neutrino and the gravitino (Abazajian & Koushiappas 2006; Boyarsky et al. 2009a), whose presence is also motivated by particle theory (e.g. Dodelson & Widrow 1994; Buchmüller et al. 2007; Takayama & Yamaguchi 2000).

Non-zero thermal velocities for WDM particles lead to a strong suppression of the linear matter power spectrum on galactic and sub-galactic scales (Bond et al. 1980; Pagels & Primack 1982; Dodelson & Widrow 1994; Hogan & Dalcanton 2000; Zentner & Bullock 2003; Abazajian 2006; Viel et al. 2005), and erase all primordial density perturbations smaller than their free-streaming scale  $\lambda_{fs}$ . Below this scale no structure is expected to form, at least not in the usual bottom-up scenario. However, the

\* E-mail: maccio@mpia.de

effective suppression of halo formation already happens well above  $\lambda_{fs}$  and is entirely described by the WDM particle mass (see Smith & Markovic 2011, and references therein).

Recent observational constraints coming from X-ray background measurements and Ly- $\alpha$  forest analysis set the allowed mass interval roughly between 2 and 50 keV (e.g. Viel et al. 2005; Seljak et al. 2006; Abazajian & Koushiappas 2006; Boyarsky et al. 2009b,c)<sup>1</sup> As a complementary study Macciò & Fontanot (2010, see also Polisensky & Ricotti 2011) compared the subhalo abundance of a Milky Way like object in different numerical warm dark matter realizations with observed satellite galaxies reported by the SDSS data and set a lower bound for a thermalized particle of  $m_{\text{WDM}} \gtrsim 2$  keV.

Another important characteristic of a WDM scenario is the possibility to *naturally* obtain cored matter density profiles. According to Liouville's theorem for collisionless systems, the finite phase space density of the cosmic fluid stays constant through cosmic history. In WDM the dark matter fluid is described by a Fermi-Dirac distribution, whose absolute value is fixed at the time of decoupling when the fluid becomes collisionless. Structure formation then happens through a complex process of distortion and folding of the phase space sheet. Since it is not possible to measure this fine-grained phase space density in simulations, one usually defines a coarse-grained or pseudo phase space density (e.g. Taylor & Navarro 2001)

$$Q \equiv \frac{\rho}{\sigma^3}, \quad (1)$$

where  $\rho$  is the mean density and  $\sigma$  is the one-dimensional velocity dispersion within some small patch of the simulation. The quantity  $Q$  corresponds to an average density of a small (but not microscopic) phase space volume and is not constant anymore. However, because of the way the phase space sheet is distorted, the value of  $Q$  can only decrease during structure formation and will never exceed its initial value set at decoupling (Dalcanton & Hogan 2001). This fundamental upper limit also holds for the local phase space density within virialised haloes at redshift zero and has a direct consequence on the density profile in real space. Since the velocity dispersion does not grow in the inner part of a halo, the real space density profile must become constant with a core size depending on the specific WDM model (Tremaine & Gunn 1979).

Due to this effect of core formation, the WDM scenario has been suggested as a solution to the long standing core-cusp problem of dwarf galaxies. In fact, observational measurements favor cored dark matter profiles in low surface brightness galaxies within the local group (Salucci et al. 2011; Kuzio de Naray & Kaufmann 2011). However, previous theoretical/analytical studies argue that the cores produced by warm dark matter might be too small to explain the observations (Kuzio de Naray et al. 2010; Villaescusa-Navarro & Dalal 2011).

Numerical N-body simulations have been used to

better understand the properties of virialized objects in the Warm Dark Matter scenarios (e.g. Bode et al. 2001; Knebe et al. 2003; Wang & White 2007; Zavala et al. 2009; Tikhonov et al. 2009; Schneider et al. 2011). High resolution simulations of single objects have studied the suppression of the galactic satellite formation due to free streaming (e.g. Colín et al. 2000; Götz & Sommer-Larsen 2002; Knebe et al. 2008; Macciò & Fontanot 2010), in order to reconcile the observed dwarf galaxy abundance with the prediction from Dark Matter based theories. More recently Colín et al. (2008) used N-body simulations to study the effects of primordial (thermal) velocities on the inner structure of dark matter haloes, with particular attention on the formation of a possible central density core. They used thermal velocities of the order of 0.1 and 0.3 km/s, without linking them to any particular WDM model, since the aim of their work was to explore the general effect of relic velocities of the DM structure. Unfortunately their combination of resolution and choice for relic velocities was not sufficient to directly test simulation results against core radii predicted by phase-space constraints.

In this work we want to extend and improve on these previous studies. We will use high resolution N-body simulations to explore the sizes of density cores in WDM and their dependence on the WDM candidate mass<sup>2</sup>. We will explore several models for WDM ranging from 2 to 0.05 keV. We will consider separately the effects of a warm dark matter candidate on the power spectrum and on the relic velocities, trying to disentangle the various consequences of these two different components. Our higher numerical resolution will allow us to directly see the formation of a density core, with a size well above the numerical resolution for the warmer candidates. We will then revise the theoretical arguments for the formation of cored profiles in WDM and perform a direct comparison between the core sizes in our simulations and the ones predicted from phase space constraints.

The paper is structured as follows: In section 2 we discuss the setup of our simulations and the way we implement thermal velocities. Section 3 is dedicated to the presentation of our results in terms of the phase space limit and its influence on the density profile of dark matter haloes. A conclusion and a summary of our work is finally given in section 3.

## 2 SIMULATIONS

Numerical simulations have been carried out using PKDGRAV, a treecode written by Joachim Stadel and Thomas Quinn (Stadel 2001). The initial conditions are generated with the GRAFIC2 package (Bertschinger 2001). All simulations start at redshift  $z_i = 99$  in order to ensure a proper treatment of the non linear growth of cosmic structures.

The cosmological parameters are set as follows:  $\Omega_\Lambda=0.727$ ,  $\Omega_m=0.273$ ,  $\Omega_b=0.044$ ,  $h = 0.7$  and  $\sigma_8 = 0.8$ ,

<sup>1</sup> In some of these analysis the warm dark matter particle is assumed to be a resonantly produced sterile neutrino (Shi & Fuller 1999). We have converted these mass limits into limits for a fully thermalized particle, such as the gravitino, using the formula provided by Viel et al. (2005).

<sup>2</sup> In the present work we only considered a very simple WDM model; it is worth commenting that there are more complex and physically motivated models discussed in the literature (e.g. warm+cold dark matter, Boyarsky et al. (2009d) or composite dark matter Khlopov (2006); Khlopov & Kouvaris (2008))

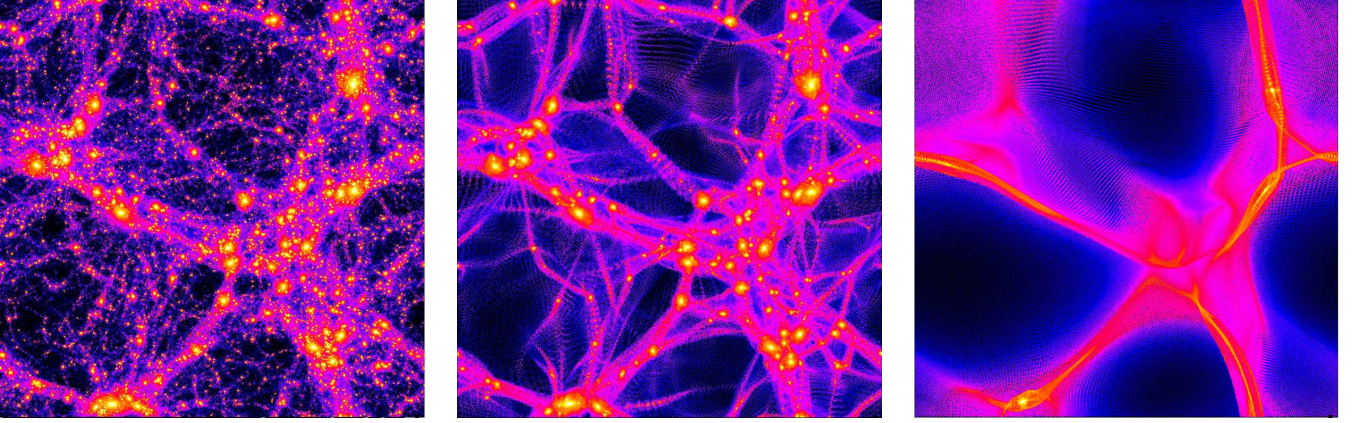


**Figure 1.** Density map of the large scale (low resolution) simulations ( $L=40$  Mpc) at redshift zero. From left to right: CDM, and two WDM with a cut in the power spectrum for a  $m_\nu$  mass of 0.2 and 0.05 keV respectively. These last two simulations have not been used in this paper and are presented only for illustration purposes, see section 2.1 for more information.

and are in good agreement with the recent WMAP mission results (Komatsu et al. 2011).

We start by running large scale simulations of a cosmological cube of side 40 Mpc, using  $2 \times 256^3$  dark matter particles. This was done for two different models, a standard LCDM and a Warm Dark Matter model with a warm candidate of mass 2 keV produced in thermal equilibrium.

To compute the transfer function for WDM models we used the fitting formula suggested by Bode et al. (2001):

$$T^2(k) = \frac{P^{\text{WDM}}}{P^{\text{CDM}}} = [1 + (\alpha k)^{2\nu}]^{-10/\nu} \quad (2)$$

where  $\alpha$ , the scale of the break, is a function of the WDM parameters, while the index  $\nu$  is fixed. Viel et al. (2005) (see also Hansen et al. 2002), using a Boltzmann code simulation, found that  $\nu = 1.12$  is the best fit for  $k < 5 h \text{ Mpc}^{-1}$ , and they obtained the following expression for  $\alpha$ :

$$\alpha = 0.049 \left( \frac{m_x}{1 \text{ keV}} \right)^{-1.11} \left( \frac{\Omega_\nu}{0.25} \right)^{0.11} \left( \frac{h}{0.7} \right)^{1.22} h^{-1} \text{ Mpc}. \quad (3)$$

We used the expression given in Eq. (3) for the damping of the power-spectrum for simplicity and generality. More accurate expressions for the damping of sterile neutrinos exist (e.g. Abazajian 2006) and show that the damping depends on the detailed physics of the early universe in a rather non-trivial way. The initial conditions for two simulations have been created using the same random phases, this means that there is a one-to-one correspondence between CDM and WDM haloes.

We then select one candidate halo with a mass similar to our Galaxy ( $M \sim 10^{12} M_\odot$ ) and re-simulated it at higher resolution. These high resolution runs are  $8^3$  times more resolved in mass than the initial ones: the dark matter particle mass is  $m_p = 1.38 \times 10^5 M_\odot$ , where each dark matter particle has a spline gravitation softening of 355 pc. This single halo has been re-simulated in several different models, all simulations are summarized in Table 1 and three of the simulations are shown in Figure 1.

**Table 1.** Simulations parameters

Label	$m_\nu$ (keV)	$m_{\nu, \text{vel}}$ (keV)	$N_{\text{vir}}$ ( $10^6$ )	$M_{\text{vir}}$ ( $10^{12} M_\odot$ )
CDM	$\infty$	–	10.2	1.42
WDM1	2.0	2.0	8.6	1.22
WDM2	2.0	0.5	8.4	1.20
WDM3	2.0	0.2	8.5	1.21
WDM4	2.0	0.1	6.7	0.93
WDM5	2.0	0.05	4.9	0.71

## 2.1 Streaming velocities

Particles that decouple whilst being relativistic are expected to retain a thermal velocity component. This velocity can be computed as a function of the WDM candidate mass ( $m_\nu$ ) according to the following expression (Bode et al. 2001):

$$\frac{v_0(z)}{1+z} = .012 \left( \frac{\Omega_\nu}{0.3} \right)^{\frac{1}{3}} \left( \frac{h}{0.65} \right)^{\frac{2}{3}} \left( \frac{1.5}{g_X} \right)^{\frac{1}{3}} \left( \frac{\text{keV}}{m_\nu} \right)^{\frac{4}{3}} \text{ km s}^{-1} \quad (4)$$

where  $z$  is the redshift. The distribution function is  $(e^{p/T_\nu} + 1)^{-1}$  until the gravitational clustering begins (Bode et al. 2001).

This formalism is correct for the “real” dark matter elementary particles (e.g. a sterile neutrino). In the N-body approach we use macro particles (with masses of the order of  $10^5 M_\odot$ ) to describe the density field. These macro particles effectively model a very large number of micro particles. Given that the velocities described in Eq. (4) have a random direction the total velocity of the macro (Nbody) particles should effectively be zero. Hence, it is not correct to directly use Eq. (4) to assign “thermal” velocities to simulation particles.

On the other hand, the net effect of the thermal velocities is to create a finite upper limit in the phase-space distribution (PSD) due to their initial velocity dispersion ( $\sigma$ ). What we are interested in is to recreate the same PSD limit in our simulation, and then study its effects on the dark matter halo density distribution. In order to achieve this goal we proceed in the following way. From Eq. (4) we

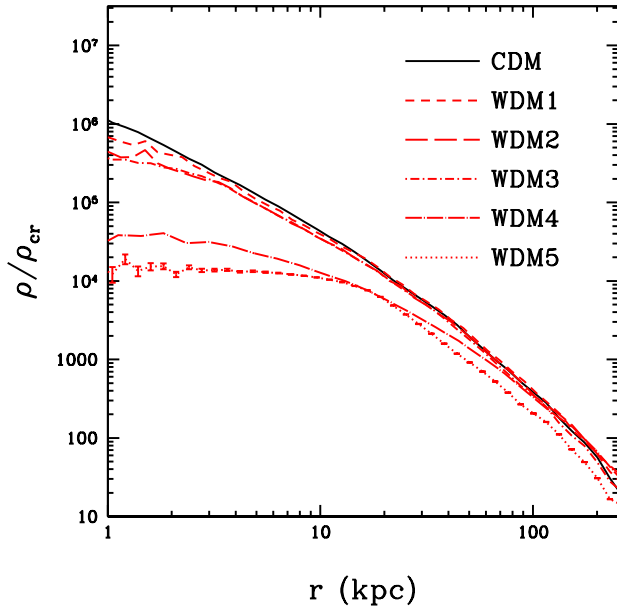


**Figure 2.** The spherically averaged density profiles for CDM, WDM1-5 haloes.

compute the rms velocity:  $\sigma(z) = 3.571v_0(z)$ , we then create a Gaussian distribution centered on zero and with the same rms  $\sigma$ . Finally we randomly generate particle velocities from this distribution and assign them to our macro particles.

As detailed in section 3.1, there is a direct connection between  $m_\nu$  and the expected size of the dark matter distribution core. This core is only due to the presence of thermal velocities and not, in first approximation, to the cut in the power spectrum described by Eq. (2). Cutting the power spectrum changes the merger history of the dark matter halo but does not affect the density profile significantly (Moore et al. 1999). This implies that in order to study the effect of different values of  $m_\nu$  (and hence  $v_0$ ) it is sufficient to “play” with Eq. (4) leaving all other simulation parameters unaltered. Following this approach we have generated several simulations using the same cut in the power spectrum ( $m_\nu$ ) but different initial thermal velocities ( $m_{\nu,\text{vel}}$ ), as detailed in Table 1.

### 3 RESULTS

Density profiles for the cold dark matter run and the four warm dark matter realizations (WDM1-WDM5) are shown in Fig. 2. The profiles show a monotonic decrease of the central density as a function of the temperature of the dark matter candidate. Cold candidate show the usual cuspy behavior (e.g. Dubinski & Carlberg 1991), while warmer candidates present a lower central density that becomes a clear core for  $m_{\nu,\text{vel}} = 0.05$  keV, with a size of several kpc.

Fig. 3 shows the time evolution of the density profile in the WDM5 simulation. The core is already in place at high redshift  $z = 1.6$ , and does not evolve substantially until  $z = 0$ . The profile only changes at large radii ( $r > 50$ ) kpc, as a consequence of the assembly of the external part of the

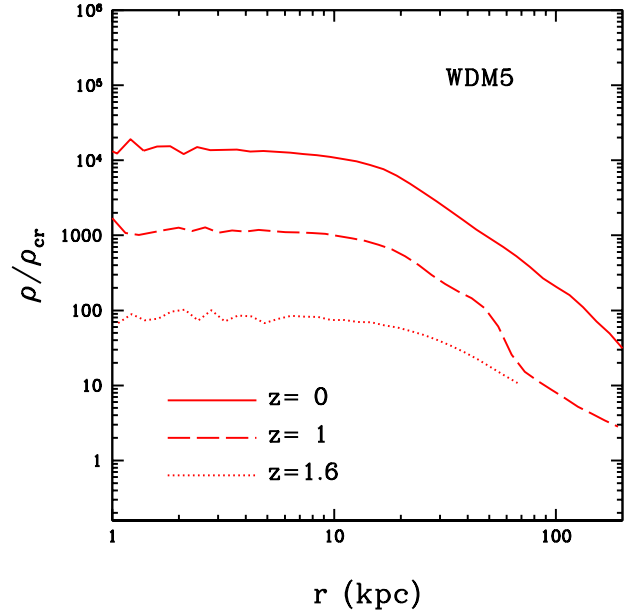


**Figure 3.** Time evolution of the density profiles for the WDM5 halo.

halo that is consistent with a typical CDM halo in the outer regions.

As already mentioned the theoretical explanation for the formation of a core is related to the presence of a maximum in the phase space density distribution. This maximum is clearly visible in Fig. 4, where we plot the phase space density proxy  $Q \equiv \rho/\sigma^3$ , for three different models, namely CDM, WDM3 and WDM5. For this latter model the phase-space proxy  $Q$  shows a large core that extends about 10 kpc. The WDM3 model also shows a strong flattening of the  $Q$  profile, consistent with a core distribution. On the other hand the CDM phase-space distribution is well fitted by a single power law profile on the whole range, in agreement with previous results Schmidt et al (2008).

Figure 5 shows the time evolution of the PSD for our warmest candidate (i.e. thermal velocities for a 0.05 keV mass particle). The solid (blue) line shows the  $Q$  radial profile in the initial conditions ( $z = 99$ ). This value has been calculated using only high resolution particles that end up within 1.5 times the virial radius of the halo at  $z = 0$ . These particles define a lagrangian region with a comoving volume of about  $(6\text{Mpc})^3$ . The other (red) lines represent the PSD profile at different redshifts (from 1.6 to 0) and have been computed using all particles within the virial radius of the halo. All quantities in the plot are in physical units. The phase space distribution shows very weak evolution with almost no evolution at all from  $z = 99$  to  $z = 1.6$ . In the same plot we also show the theoretical maximum phase-space density achievable by this model (see Eq. (7) for a rigorous definition of  $Q_{\text{max}}$ ). As we will see later (in section 3.1) the value of this maximum phase space density depends on the local value of  $\Omega_m$ . The two (black) lines show predictions for  $Q_{\text{max}}$  for the average matter density in our simulation ( $\Omega_m = 0.273$ ) and for its *local* value, which we measured by dividing the mass contained in the halo lagrangian region

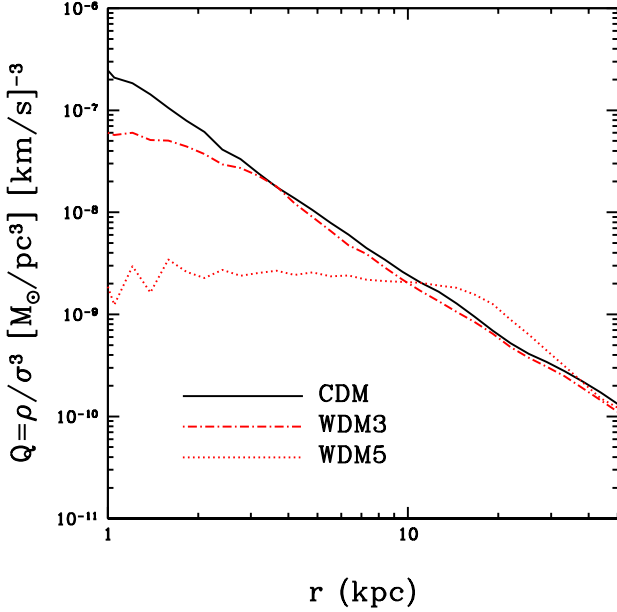


**Figure 4.** Phase space density profile for the CDM, WDM3 and WDM5 models at  $z = 0$ .

(defined above) by its volume. This local matter density parameter turned out to be  $\Omega_{m,local} = 0.0344$ <sup>3</sup>.

This second theoretical prediction, that took into account the local value of the matter density parameter, is in very good agreement with the simulation results. It also shows that global prediction on the size of cores in WDM could be affected by the local overdensity. We will come back to this issue later.

In order to quantify the flatness (and the core size) of WDM profiles we have fitted all our density profiles with the following parametric description, originally presented in Stadel et al. (2009):

$$\rho(r) = \rho_0 \exp(-\lambda[\ln(1 + r/R_\lambda)]^2). \quad (5)$$

In this parameterization the density profile is linear down to a scale  $R_\lambda$  beyond which it approaches the central maximum density  $\rho_0$  as  $r \rightarrow 0$ . We also note that if one makes a plot of  $d \ln \rho / d \ln(1 + r/R_\lambda)$  versus  $\ln(1 + r/R_\lambda)$  then this profile forms an exact straight line with slope  $2\lambda$ .

This fitting function is extremely flexible and makes possible to reproduce at the same time both cuspy profiles like the one predicted by the CDM theory, as well as, highly cored profiles, like in the WDM5 case (as shown in Fig. 6). The values of the parameter are obtained via a  $\chi^2$  minimization procedure using the Levenberg & Marquart method. From now on we will use the value of the fitting parameter  $R_\lambda$  as the fiducial value of the central density core in simulated profiles ( $r_{core,s}$ , hereafter). The  $r_{core,s}$  values for all our haloes are reported in the first column of Table 2.

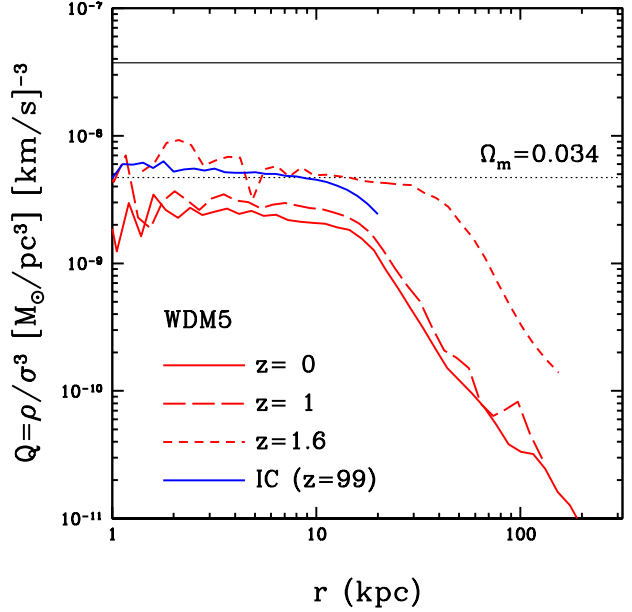


**Figure 5.** Time evolution of the PSD radial profile for the WDM5 model. The two (black) lines represent the theoretical prediction for the maximum value of  $Q$  according to equation 7. The upper one is for the global value of the matter density parameter ( $\Omega_m$ ) while the lower one is for its local value ( $\Omega_{m,local} = 0.0344$ , See text for more details).

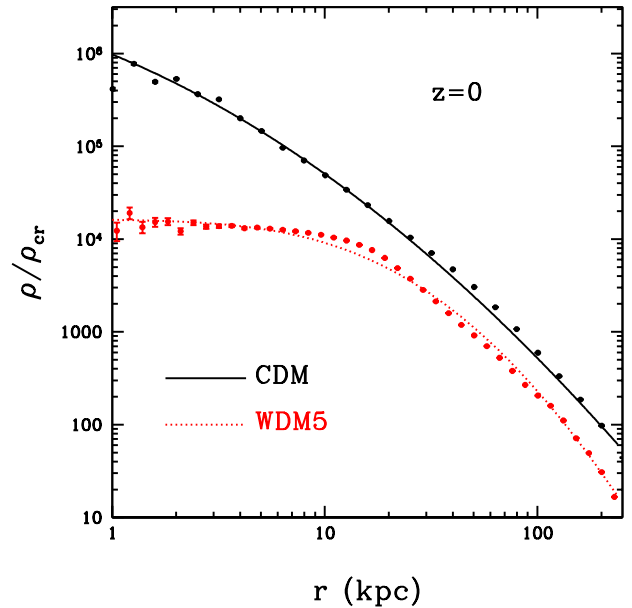


**Figure 6.** Density profiles for CDM and WDM5 and their fit using Eq. (5).

<sup>3</sup> This low value is not surprising since the mass of the halo with  $1.5 R_{vir}$  is of the order of  $5 \times 10^{12} M_\odot$  and it is distributed on a volume of  $(6 \text{ Mpc})^3$  in the IC. This is partially a consequence of having chosen in our study a very isolated halo

### 3.1 Comparison with theoretical predictions

In Tremaine & Gunn (1979, TG79 hereafter) limits on the mass of a neutrino are derived from the maximum phase space density of a homogeneous neutrino background, with the further assumptions that neutrinos form bound structures and that their central regions can be well-approximated by an isothermal sphere.

Assuming a Maxwellian velocity distribution they obtained the maximum phase space density:

$$Q_{max} \equiv \frac{\rho}{\sigma^3} \propto m_\nu^4 \quad (6)$$

where  $m_\nu$  is the mass of the (warm) dark matter candidate. This limit has been then used in several follow up papers to estimate the size of density cores in warm dark matter haloes (e.g. Dalcanton & Hogan 2001; Strigari et al. 2006).

While the calculation from TG79 is formally correct, it cannot be directly applied to our numerical simulations (and more in general to any numerical simulation). The reason is that when deriving  $Q_{max}$ , TG79 tried to constrain *at the same time* both the phase space density and the total matter density ( $\Omega_m$ ) in warm (or hot) dark matter. In doing that they correctly assumed  $\Omega_{WDM} \propto m_\nu$ . This is not what is usually done in cosmological simulations, where the value of  $\Omega_m$  is kept constant among different models (e.g. CDM *vs* WDM) and fixed to match cosmic micro wave based results.

It is then worthwhile calculating the value of  $Q_{max}$  under the assumption of a fixed value for the total dark matter density. We can start from the definition of  $Q$ :

$$Q_{max} \equiv \frac{\rho}{\sigma^3} = \frac{\Omega_m \rho_{cr}}{\sigma^3} \quad (7)$$

where  $\rho_{cr} = 2.775 \times 10^{11} h^2 M_\odot \text{Mpc}^{-3}$  is the critical density of the Universe. Following TG79 we can rewrite the denominator according to:

$$\sigma = \frac{kT_\nu}{cm_\nu} \quad (8)$$

The temperature of the WDM particle ( $T_\nu$ ) can be computed from the temperature of the photons if the WDM candidate has a mass below 1 MeV (e.g. Weinberg 1972), this gives:

$$T_\nu = \left(\frac{4}{11}\right)^{1/3} T_\gamma = 1.9K \quad (9)$$

If we now combine Eqs. (7), (8) and (9) we obtain a new expression for maximum phase space density:

$$Q_{max} = 2.74 \times 10^{-4} \left(\frac{m_\nu}{\text{keV}}\right)^3 \left(\frac{\Omega_m}{0.25}\right) \left(\frac{h}{0.7}\right) \frac{M_\odot \text{pc}^{-3}}{(\text{km s}^{-1})^{-3}}. \quad (10)$$

Aside from numerical factors, the most important difference with respect to the expression derived by TG79, is the different scaling of  $Q$  with the WDM particle mass, a direct consequence of assuming a fixed (WDM mass independent) matter density parameter  $\Omega_m$ .

Finally the maximum phase space density can be converted in a 'core' size following Hogan & Dalcanton (2000):

$$r_{\text{core,t}}^2 = \frac{\sqrt{3}}{4\pi G Q_{max}} \frac{1}{<\sigma_{halo}^2>^{1/2}}. \quad (11)$$

where  $\sigma_{halo}$  is the velocity dispersion (i.e. the mass) of the

**Table 2.** Size of density cores using different methods. See text for a more detailed explanation

Label	$r_{\text{core,s}}$ (kpc)	$r_{\text{core,Q}}$ (kpc)	$r_{\text{core,t}}$ (kpc)
CDM	< 0.4	< 0.4	$\infty$
WDM1	< 0.4	< 0.4	0.009
WDM2	< 0.4	< 0.4	0.068
WDM3	0.42	< 1.1	0.272
WDM4	1.63	1.80	0.69
WDM5	4.56	4.85	2.79

simulated dark matter halo. Values of  $r_{\text{core,t}}$  for our simulated haloes are reported in the last column of Table 2.

In the following we will compare this theoretical value of the core ( $r_{\text{core,t}}$ ) with two different core sizes than can be estimated directly from the simulations. The first one is given by the  $R_\lambda$  parameter obtained by fitting the numerical density profile, as shown in Fig. 6 and we will refer to this value as  $r_{\text{core,s}}$ . The second one is obtained by computing  $Q_{max}$  from the simulated density profile (as shown in Fig. 4) and then inserting this value in Eq. (11), we named this second parameter  $r_{\text{core,Q}}$ .

Results for the three definitions of the core size for all our simulations are summarized in Table 2. Overall the three different estimators for the core size are in fairly good agreement.  $r_{\text{core,Q}}$  gives on average a larger value for the core, for the WDM4 and WDM5 runs, while for the WDM3 simulation is only able to give an upper value, since there is not a clear indication of convergence towards a maximum value in the  $Q_{max}$  profile, as shown in Fig. 4.

Fig. 7 shows the comparison of the cored found directly in simulations ( $r_{\text{core,s}}$ ) with the core predicted by the above simple theoretical argument ( $r_{\text{core,t}}$ ). In the plot there are three independent theoretical predictions for the core value. The solid and dashed lines are obtained from Eqs. (11) and (10), using two different values for the matter density parameter  $\Omega_m$ , namely the global one (0.273) and the local one (0.034). Overall numerical results for WDM3, WDM4 and WDM5 are in very good agreement with the theoretical expectations from Eqs. (11) and (10). The WDM1 and WDM2 simulations only put upper limits on the size of the core, since the values of  $R_\lambda$  we obtain from fitting the density profile fall below the simulation softening (the dashed black line in the figure). The plot also shows that using the local value of the density parameter gives a better fit to the data. On the other hand the core size only depends on the square root of  $\Omega_m$ , so the difference between the two core size predictions is not very large. A third theoretical value (dotted line) is determined using the original argument by TG79, where the matter density parameter is linked to the mass of the warm candidate. In this case the theoretical relation seems to be "tilde" with respect the simulation results, and it tends to over estimate the size of the density core in simulations with a fixed  $\Omega_m$  parameter.

Using our new determination of the core size as a function of the warm dark matter mass we compute the expected value of  $r_{\text{core}}$  for the typical halo mass ( $5 \times 10^8 M_\odot$ , see Macciò et al. (2010)) of dwarf galaxies orbiting the Milky-Way. Results are shown in Fig. 8: the grey shaded area takes



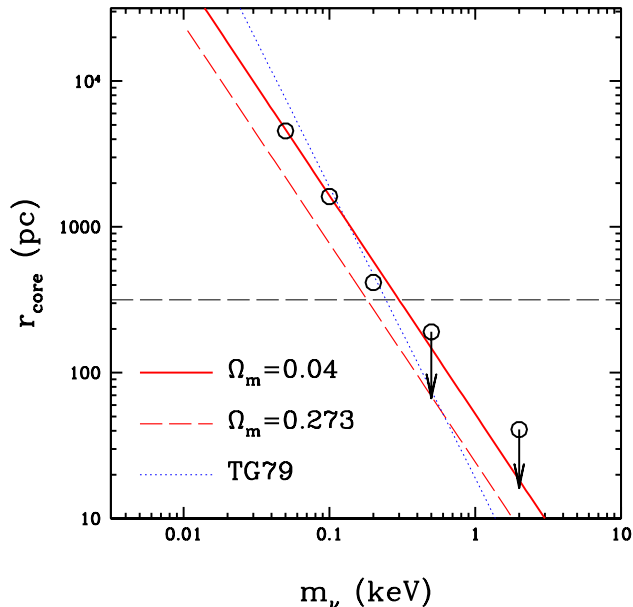


**Figure 7.** Comparison between core size in simulations (open symbols) and the theoretical expectation for a  $M = 10^{12} M_{\odot}$  halo (solid line). The dashed line is the gravitational softening of our simulations. All points below this line should be considered as upper limits on the core size.

into account possible different values of the local matter density parameter in the range  $0.05 < \Omega_m < 1.4$ .

From the figure it is clear that a core of  $\approx 1$  kpc would require a wdm mass of the order of 0.1 keV, well below current observational limits from large scales.

If we assume a warm dark matter particle mass of  $m_{\nu} \sim 2$  keV (represented by the dashed vertical line), in agreement with several astrophysical constraints (e.g. Viel et al. 2008), the maximum core size we can expect ranges from 10 pc for a massive, MW-like halo (see also figure 7), to 30-50 pc for a dwarf galaxy like halo. Finally, in predicting the core size for satellite galaxies in the MW halo, it must be taken into account that due to stripping and tidal forces satellites can lose significant mass after accreting into larger haloes (e.g. Penarrubia et al. 2008; Macciò et al. 2010). This implies that the halo mass we may infer today for those galaxies is only a lower limit on the mass they had before accretion, which is the one to be used (as  $\sigma_{halo}^2$ ) in Eq. 11.

#### 4 CONCLUSIONS

We have used high resolution N-body simulations to examine the effects of free streaming velocities on halo internal structure in warm dark matter models. We find:

- The finite initial fine grained PSD is also a maximum of the coarse grained PSD, resulting in PSD profiles of WDM haloes that are similar to CDM haloes in the outer regions, however they flatten towards a constant value in the inner regions. This is in agreement with previous studies based

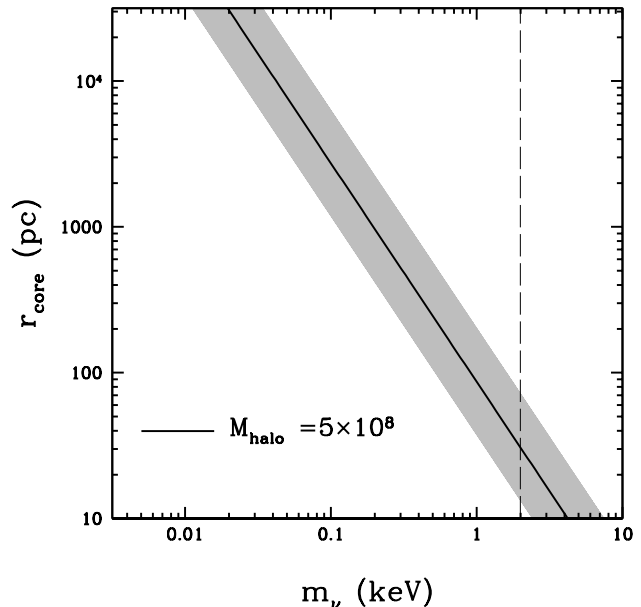


**Figure 8.** Expected core size for the typical dark matter mass of Milky Way satellites as a function of the WDM mass  $m_{\nu}$ . The shaded area takes into account possible different values of the local density parameter  $0.05 < \Omega_m < 1.4$ . The vertical dashed line shows the current limits on the WDM mass from large scale structure observations.

on simulations (Colín et al. 2008) and theoretical arguments Villaescusa-Navarro & Dalal (2011).

- The finite PSD limit results in a constant density core with characteristic size that is in agreement with theoretical expectations i.e. following Tremaine & Gunn 1979, especially if value of the local matter density is taken into account.

- The core size we expect for thermal candidates allowed by independent constraints on large scales (Lyman- $\alpha$  and lensing,  $m_{\nu} \approx 1 - 2$  keV), is of the order of 20-60 pc. This is not sufficient to explain the observed cores in dwarf galaxies that are around kpc scale (Walker & Penarrubia 2011; Jardel & Gebhard 2012).

- Our results show that a core around kpc scale in dwarf galaxies, would require a thermal candidate with a mass below 0.1 keV, ruled out by all large scale structure constraints (Seljak et al. 2006; Miranda & Macciò 2007; Viel et al. 2008). Moreover with such a warm candidate, the exponential cut-off of the Power Spectrum would make impossible to obtain these dwarf galaxies in the first place (e.g. Macciò & Fontanot 2010).

- All together these results lead to a nice “Catch 22” problem for warm dark matter: *If you want a large core you won’t get the galaxy, if you get the galaxy it won’t have a large core.*

We conclude that the solution of the cusp/core problem in local group galaxies cannot completely reside in simple models (thermal candidates) of warm dark matter. If cores are required then it seems that baryonic feedback (e.g. Governato et al. 2010; Macciò et al. 2012) is still the most likely way to alter the density profile of dark matter and

hence reconcile observations with cold/warm dark matter predictions.

## ACKNOWLEDGMENTS

We acknowledge stimulating discussions with George Lake, Jürg Diemand and Justin Read. Numerical simulations were performed on the THEO and PanStarrs2 clusters of the Max-Planck-Institut für Astronomie at the Rechenzentrum in Garching and on the zBox3. S. P. would like to thank Joachim Stadel and Doug Potter for their crucial contribution to this project.

## REFERENCES

- Abazajian, K. & Koushiappas, S. M., 2006, *Phys.Rev.D*, 74, 023527
- Abazajian, K. 2006, *Phys.Rev.D*, 73, 063506
- Bertschinger, E., 2001, *ApJS*, 137, 1
- Bode, P., Ostriker, J. P. & Turok, N., 2001, *ApJ*, 556, 93
- Bond, J. R., Efstathiou, G., & Silk, J. 1980, *Physical Review Letters*, 45, 1980
- Boyarsky, A., Ruchayskiy, O. & Shaposhnikov, M., 2009, *Annual Review of Nuclear and Particle Science*, 59, 191
- Boyarsky, A., Lesgourgues, J., Ruchayskiy, O. & Viel, M., 2009a, *Journal of Cosmology and Astro-Particle Physics*, 5, 12
- Boyarsky, A., Ruchayskiy, O. & Iakubovskyi, D., 2009, *JCAP*, 0903
- Boyarsky, A., Lesgourgues, J., Ruchayskiy, O. & Viel, M., 2009b, *Physical Review Letters*, 102, 201304
- Buchmüller, W., Covi, L., Hamaguchi, K., Ibarra, A. & Yanagida, T., 2007, *JHEP*, 03, 037
- Colín, P., Avila-Reese, V. & Valenzuela, O., 2000, *ApJ*, 542, 622
- Colín, P., Valenzuela, O. & Avila-Reese, V., 2008, *ApJ*, 673, 203
- Dalcanton, J. J. & Hogan, C. J., 2001, *ApJ*, 561, 35
- de Blok, W. J. G., McGaugh, S. S., Bosma, A., & Rubin, V. C. 2001, *ApJL*, 552, L23 =
- Diemand, J., Zemp, M., Moore, B., Stadel, J., & Carollo, M. 2005, *MNRAS*, 364, 665
- Dodelson, S. & Widrow, L. M. 1994, *Physical Review Letters*, 72, 17
- Dubinski, J. & Carlberg, R. G. 1991. *Astrophysical Journal*, 378, 496
- Flores, R. A. & Primack, J. R. 1994, *ApJL*, 427, L1
- Governato, F., Brook, C., Mayer, L., Brooks, A., Rhee, G., Wadsley, J., Jonsson, P., Willman, B., Stinson, G., Quinn, T. & Madau, P., 2010, *Nature*, 463, 203
- Götz, M., Sommer-Larsen, J. 2002 *ApSS*, 281, 415
- Hansen, S. H., Lesgourgues, J., Pastor, S. & Silk, J., 2002, *MNRAS*, 333, 546
- Hogan, C. J. & Dalcanton, J. J. 2000, *Phys.Rev.D*, 62, 063511
- Jardel, J. & Gebhardt, K., 2012, *ApJ*, in press
- Khlopov, M. Y., 2006, *JETP Lett.*, 83,1
- Khlopov, M. Y. & Kouvaris, C., 2008, *Phys.Rev.D*, 78, 065040
- Klypin, A., Kravtsov, A. V., Valenzuela, O., & Prada, F. 1999, *ApJ*, 522, 82
- Knebe, A., Devriendt, J. E. G., Gibson, B. K., & Silk, J. 2003, *MNRAS*, 345, 1285
- Knebe, A., Arnold, B., Power, C., & Gibson, B. K. 2008, *MNRAS*, 386, 1029
- Komatsu, E., Smith, K. M., Dunkley, J., & The WMAP Team, 2011, *ApJS*, 192, 18
- Kuzio de Naray, R. & Kaufmann, T., 2011, *MNRAS*, 414, 3617
- Kuzio de Naray, R., Martinez, J. D., Bullock, J. S., Kaplinghat, M., 2010, *ApJL*, 710, L161
- Kuzio de Naray, R., McGaugh, S. S., & Mihos, J. C. 2009, *ApJ*, 692, 1321
- Macciò A. V., Dutton A. A., van den Bosch F. C., Moore B., Potter D., Stadel J., 2007, *MNRAS*, 378, 55
- Macciò, A. V., Kang, X., Fontanot, F., Somerville, R. S., Kopev, S. E. & Monaco, P., 2010, *MNRAS*, 402, 1995
- Macciò, A. V. & Fontanot, F., 2010, *MNRAS*, 404, L16
- Macciò, A. V., Stinson, G., Brook, C. B., Wadsley, J., Couchman, H. M. P., Shen, S., Gibson, B. K. & Quinn, T., 2012, *ApJ*, 744, L9
- Miranda, M. & Macciò, A. V., 2007, *MNRAS*, 382, 1225
- Moore, B. 1994, *Nature*, 370, 629
- Moore, B., Ghigna, S., Governato, F., Lake, G., Quinn, T., Stadel, J., & Tozzi, P. 1999, *ApJL*, 524, L19
- Navarro, J. F., Frenk, C. S. & White, S. D. M., 1997, *ApJ*, 490, 493
- Oh, S.-H., de Blok, W. J. G., Brinks, E., Walter, F., & Kennicutt, R. C., Jr. 2011, *AJ*, 141, 193
- Pagels, H. & Primack, J. R. 1982, *Physical Review Letters*, 48, 223
- Peebles, P. J. E. & Nusser, A., 2010, *Nature*, 465, 565
- Penarrubia, J., Navarro, J. F. & McConnachie, A. W., 2008, *ApJ*, 673, 226
- Polinsky, E. & Ricotti, M., 2011, *Phys.Rev.D*, 043506
- Salucci, P., Wilkinson, M. I., Walker, M. G., Gilmore, G. F., Grebel, E. K., Koch, A., Frigerio Martins, C., Wyse, R. F. G., 2011, *arXiv:1111.1165*
- Schmidt, K. B., Hansen, S. H., & Macciò, A. V. 2008, *ApJL*, 689, L33
- Schneider, A., Smith, R. E., Macciò, A. V. & Moore, B. 2011, *arXiv:1112.0330*
- Shaposhnikov, M., 2008, *Lecture from the Eleventh Marcel Grossmann Meeting*, 1006
- Seljak, U., Makarov, A., McDonald, P., & Trac, H. 2006, *Phys. Rev. Lett.*, 97, 191303
- Shi, X. & Fuller, G. M., 1999, *Physical Review Letters*, 82, 2832
- Smith, R. E. & Markovic, K. 2011, *Phys.Rev.D*, 84, 063507
- Springel, V., Wang, J., Vogelsberger, M., Ludlow, A., Jenkins, A., Helmi, A., Navarro, J. F., Frenk, C. S. & White, S. D. M., 2008, *MNRAS*, 391, 1685
- Stadel, J., 2001, *PhD Thesis*, University of Washington
- Stadel J., Pooter, D., Moore, B., Diemand, D., Madau, P., Zemp, M., Kuhlen, M. & Quilis, V., 2009, *MNRAS*, 391, L21
- Strigari, L. E., Bullock, J. S., Kaplinghat, M., Kravtsov, A. V., Gnedin, O. Y., Abazajian, K. & Klypin, A. A. 2006, *ApJ*, 652, 306
- Takayama, F. & Yamaguchi, M., 2000, *Phys. Lett. B* 485, 388



- Taylor, J. E. & Navarro, J. F. 2001, ApJ, 563, 483
- Tegmark, M., & The SDSS Team. 2006, PRD, 74, 123507
- Tikhonov, A. V., Gottlöber, S., Yepes, G. & Hoffman, Y., 2009, MNRAS, 399, 1611
- Tremaine, S. & Gunn, J. E. 1979, Phys.Rev.Let., 42, 407
- Viel, M., Lesgourgues, J., Haehnelt, M. G., Matarrese, S., & Riotto, A., 2005, Phy.Rev.D, 71, 063534
- Viel, M., Becker, G. D., Bolton, J. S., Haehnelt, M. G., Rauch, M. & Sargent, W. L. W., 2008, Physical Review Letters, 100, 041304
- Villaescusa-Navarro, F., & Dalal, N., 2011, JCAP 1103, 024
- Wang, J., White, S. D. M. 2007, MNRAS, 380, 93
- Waler, M. G. & Penarrubia, J. 2011, ApJ, 742, 20
- Weinberg, S., 1972, Wiley, *Gravitation and Cosmology*
- Zavala, J., Jing, Y. P., Faltenbacher, A., Yepes, G., Hoffman, Y., Gottlöber, S. & Catinella, B., 2009, ApJ, 700, 1779
- Zentner, A. R. & Bullock, J. S. 2003, ApJ, 598, 49